## REFERENCES AND NOTES

1. A. Hale and T. Bopp, *IAU Circular 6187* (1995).
2. D. Green, *IAU Circular 6191* (1995).
3. B. G. Marsden, *IAU Circular 6198* (1995).
4. _____, *IAU Circular 6224* (1995).
5. J. H. Oort and M. Schmidt, *Bull. Astron. Inst. Neth.* **11**, 91 (1951).
6. F. L. Whipple, *Moon Planets* **18**, 343 (1978).
7. M. F. A'Hearn, R. L. Millis, D. G. Schleicher, D. J. Osip, P. V. Birch, *Icarus* **118**, 223 (1995).
8. H. E. Matthews, D. Jewitt, M. C. Senay, *IAU Circular 6234* (1995).
9. H. Rauer *et al.*, *IAU Circular 6236* (1995).
10. A. Fitzsimmons, *IAU Circular 6252* (1995); $Q_{CN} = 6 \pm 3 \times 10^{25}$ molecules $s^{-1}$ at $r_h = 6.8$ AU [A. Fitzsimmons and I. M. Cartwright, *Mon. Not. R. Astron. Soc.* **278**, L37 (1996)].
11. $Q_{CN} = 2.5 \pm 0.5 \times 10^{25}$ molecules $s^{-1}$ at $r_h = 6.8$ AU [A. L. Cochran, *Bull. Am. Astron. Soc.* **28**, 1093 (1996); personal communication].
12. R. M. Wagner and D. G. Schleicher, *Science* **275**, 1918 (1997).
13. D. G. Schleicher, R. L. Millis, P. V. Birch, in preparation.
14. C. E. Randall, D. G. Schleicher, R. G. Ballou, D. J. Osip, *Bull. Am. Astron. Soc.* **24**, 1002 (1992); C. E. Randall and D. G. Schleicher, in preparation.
15. B. G. Marsden, *IAU Circular 6463* (1996).
16. Charge-coupled device imaging during 1996 and 1997 from Lowell Observatory by D. G. Schleicher, S. M. Lederer, R. L. Millis, T. L. Farnham, and E. Ford.
17. Z. Sekanina, *IAU Circular 6542* (1997).
18. C. W. Hergenrother and S. M. Larson, *IAU Circular 6555* (1997); J. Lecacheux, L. Jorda, F. Colas, *IAU Circular 6560* (1997).
19. D. G. Schleicher and R. L. Millis, *Astrophys. J.* **339**, 1107 (1989).
20. J. J. Cowan and M. F. A'Hearn, *Moon Planets* **21**, 155 (1979).


21. We thank D. Osip for helpful discussions and D. Thompson for obtaining some of the observations. Supported by NASA grants to Lowell Observatory and to the University of Florida.

10 February 1997; accepted 3 March 1997


# Evolution of the Outgassing of Comet Hale-Bopp (C/1995 O1) from Radio Observations


Nicolas Biver, Dominique Bockelée-Morvan,* Pierre Colom, Jacques Crovisier, John K. Davies, William R. F. Dent, Didier Despois, Eric Gérard, Emmanuel Lellouch, Heike Rauer, Raphael Moreno, Gabriel Paubert



**Spectra obtained from ground-based radio telescopes show the progressive release of CO, $CH_3OH$, HCN, $H_2O$ (from OH), $H_2S$, CS, $H_2CO$, $CH_3CN$, and HNC as comet Hale-Bopp (C/1995 01) approached the sun from 6.9 to 1.4 astronomical units (AU). The more volatile species were relatively more abundant in the coma far from the sun, but there was no direct correlation between overabundance and volatility. Evidence for $H_2O$ sublimation from icy grains was seen beyond 3.5 AU from the sun. The change from a CO-driven coma to an $H_2O$-driven coma occurred at about 3 AU. The gas outflow velocity and temperature increased as Hale-Bopp approached the sun.**


Cometary nuclei are porous bodies consisting of a mixture of ices and refractory grains. Progress made in the identification of cometary volatiles shows that ices of different volatility coexist in the nucleus (*1*). Although $H_2O$ is the dominant ice and controls cometary activity within 3 AU from the sun, the recent detection of CO in the distant comet P/Schwassmann-Wachmann 1 at millimeter wavelengths (*2*) suggested that, farther from the sun, cometary activity is driven by the sublimation of more volatile species. Questions arise as to the physical state and sublimation mechanisms of ices and the relative roles of the various volatiles in the comet's activity. Given the existence of processes causing chemical differentiation within the nucleus, an important issue is whether the molecular abundances measured in the coma near perihelion are representative of the bulk composition of the nucleus. The discovery of Hale-Bopp at heliocentric distance $r_h = 7$ AU (*3*) offered us the opportunity to address these problems observationally by following the outgassing of this exceptionally bright comet over a wide range of $r_h$.

Hale-Bopp was observed on a regular basis between August 1995 and late January 1997 with the Nançay telescope, the Institut de Radio Astronomie Millimétrique (IRAM) 30-m telescope (*4*), and the James Clerk Maxwell Telescope (JCMT) (*5*) at decimeter, millimeter, and submillimeter wavelengths, respectively. The OH lines at 18 cm were monitored at Nançay, and observations at IRAM and JCMT focused on rotational lines of parent molecules. The general goals of this campaign were to (i) observe the onset of outgassing of the different species, (ii) monitor their production rates as a function of $r_h$, and (iii) constrain the kinetic temperature and expansion velocity in the coma and their variation with $r_h$. Several transitions of the same molecule were observed simultaneously whenever possible to understand the excitation conditions in the coma and to infer the production rates.

Observations at IRAM started in mid-August 1995, when Hale-Bopp was at $r_h = 6.9$ AU (*6*). Monitoring of OH at Nançay started in December 1995, although preliminary observations had been acquired earlier (*7*). We detected more than 50 molecular lines, showing the progressive release of nine molecular species (CO, $CH_3OH$, HCN, OH, $H_2S$, $H_2CO$, CS, $CH_3CN$, and HNC) as the comet approached the sun (Table 1). With the exception of $NH_3$, OCS, HNCO, and some isotopic species, identified in comet Hyakutake (C/1996 B2) (*8*), all molecular species detected at radio wavelengths in previous comets were observed in Hale-Bopp at $r_h > 2.4$ AU. A number of species were also observed at other wavelengths. In particular, the first detection of the OH radical was actually obtained with the Hubble Space Telescope (*9*) 2 weeks before its radio detection. In addition, $CO_2$, CO, and $H_2O$ were detected at infrared wavelengths by the Infrared Satellite Observatory (*10*).

Most of the lines in our spectra were blueshifted with respect to the geocentric radial velocity of the comet (Fig. 1). Because the phase angle was always <20°, this velocity shift is indicative of anisotropic outgassing with preferred outflow from the sunward side of the nucleus. Coarse mapping of the HCN lines, performed from August to October 1996, showed enhanced outgassing ~45°N from the sun position angle. Beyond $r_h = 3.5$ AU, the OH lines were less blueshifted than the CO lines (Fig. 2A). Although to a lesser extent, the same behavior is observed at $r_h > 4$ AU for the $CH_3OH$ lines. This behavior indicates that some molecular species, such as $H_2O$ and $CH_3OH$, were partly sublimating from icy grains when observed far from the sun, in contrast to the more volatile CO molecule outgassed mainly from the nucleus. Icy grains of $H_2O$ were detected through their infrared spectral signature at 1.5 and 2.05 μm when Hale-Bopp was at $r_h = 6.8$ AU (*11*). The low Doppler shifts of the OH and $CH_3OH$ lines (that is, low bulk velocity of


N. Biver, D. Bockelée-Morvan, P. Colom, J. Crovisier, E. Gérard, E. Lellouch, H. Rauer, Observatoire de Paris-Meudon, F-92195 Meudon, France.
J. K. Davies and W. R. F. Dent, Joint Astronomy Centre, 660 North A'ohoku Place, University Park, Hilo, HI 96720–6030, USA.
D. Despois, Observatoire de Bordeaux, B.P. 89, F-33270 Floirac, France.
R. Moreno and G. Paubert, Institut de Radioastronomie Millimétrique, Avenida Divina Pastora 7, 18012 Granada, Spain.

*To whom correspondence should be addressed. E-mail: domi@mesioa.obspm.fr

the $H_2O$ and $CH_3OH$ comae, the bulk velocity being the velocity vector averaged over the whole coma and weighted by the local density) are in agreement with a population of icy grains outflowing at a velocity much lower than the CO velocity and whose whole surface sublimates. Low velocities are expected for large grains and for small grains derived from the fragmentation of larger particles. Enhanced outgassing toward the sun, which may occur for the largest nonisothermal grains, would result in significant spectral blueshifts only moderately affected by the rocket force exerted on the grains. As $r_h$ decreased, the sublimation of grains took place closer to the nucleus, and the collisional coma extended. Molecules released in the collision-dominated coma acquired the bulk average expansion velocity of the gas through conversion of translational energy. The radio observations indicate that sublimating $H_2O$ ice grains were still present in the coma at $r_h$ = 3.5 AU. Modeling of sublimation processes in Hale-Bopp (*12*) showed that the large $H_2O$ production rates observed beyond 3 AU can only be explained by evaporation from icy dust grains. The earlier disappearance of the signature of $CH_3OH$ sublimating from grains is possibly due to its higher volatility compared to $H_2O$.

The overall decrease of the CO and $CH_3OH$ Doppler blueshifts, extrapolating toward zero at perihelion (Fig. 2A), indicates a spatial distribution initially restricted to the sunward hemisphere and slowly expanding angularly through the night hemisphere. This may reflect the global increase of the temperature of the nucleus surface, which allowed CO and $CH_3OH$ sublimation over a more extended region as $r_h$ decreased. The systematic blueshift of the OH line observed down to $r_h$ = 1.4 AU would then be due to the $H_2O$ outgassing being more sensitive to diurnal temperature variations than the CO and $CH_3OH$ outgassing (*13*). An alternative explanation for the low CO Doppler shift at $r_h$ = 1.4 AU is a strong contribution of the distributed source of CO as was seen in comet P/Halley near perihelion (*14*).

The line shapes were used to estimate the gas outflow velocity and its evolution with $r_h$, a necessary parameter for the evaluation of gas production rates from line intensities (Fig. 2B). We derived the CO expansion velocity from the position of the half-peak intensity in the blue wing of the line profile (*15*). The $H_2O$ outflow velocity was derived from the OH line shapes by the trapezium method (*16*). The CO velocity follows a variation with $r_h$ close to the commonly used $r_h^{-0.5}$ dependence. The velocity extrapolates to >1 km $s^{-1}$ at $r_h$ = 1 AU, in agreement with previous measurements in other active comets (*16*, *17*). The

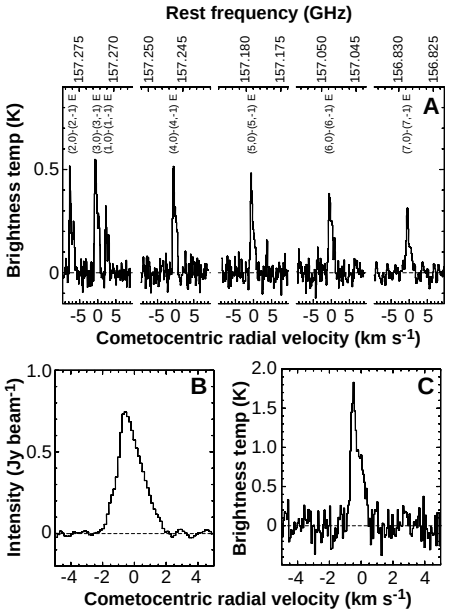


**Fig. 1.** A selection of radio spectra of Hale-Bopp. (**A**) The 157-GHz group of lines of $CH_3OH$ observed on 10 November 1996 at IRAM. The rotational lines are labeled according to the (*J*, *k*) A/E notation for the torsion-rotation levels of $CH_3OH$ (*26*). (**B**) Average of the 1667- and 1665-MHz lines of the OH radical (scaled to 1667 MHz) observed from 17 to 30 November 1996 at the Nançay radio telescope (1 Jy = $10^{-2}$ W $m^{-2}$ $Hz^{-1}$). (**C**) The *J*(3-2) CO line at 345 GHz observed on 28 to 29 July 1996 at JCMT. The lower horizontal axis is the radial velocity with respect to the comet rest velocity projected on the line of sight.

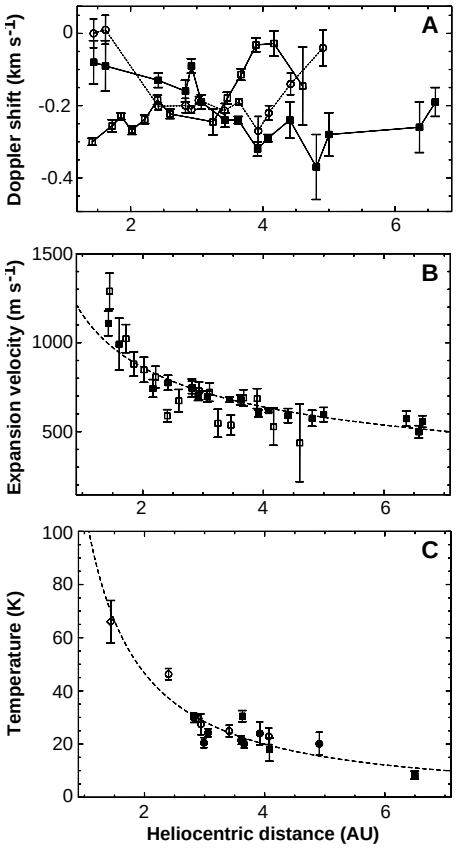


**Fig. 2.** Evolution of some coma parameters with heliocentric distance $r_h$. (**A**) Doppler shift of the CO (filled squares), $CH_3OH$ (open circles), and OH (open squares) lines (*27*). (**B**) Expansion velocity $V_{exp}$ of CO (filled squares) and $H_2O$ (open squares), derived from the line shapes of CO and OH, respectively (*27*). The dashed line is a power-law fit [$V_{exp} = (1.16 \pm 0.08) r_h^{(-0.43 \pm 0.02)}$ km $s^{-1}$] to the CO velocity from 6.6 to 1.4 AU. (**C**) Rotational temperatures derived from the relative intensities of the CO lines (115, 230, 345, and 460 GHz) (filled squares), the $CH_3OH$ 157-GHz multiplet (open circles), and the $CH_3OH$ 304/307-GHz pair (filled circles). These rotational temperatures should be close to the gas kinetic temperature. The value at $r_h$ = 1.44 AU (open diamond, far left) is the gas kinetic temperature derived from the rotational temperature of 53 ± 6 K of the 252-GHz $CH_3OH$ lines. The dashed line is the power law fit $T = (109 \pm 35) r_h^{(-1.22 \pm 0.07)}$ K.

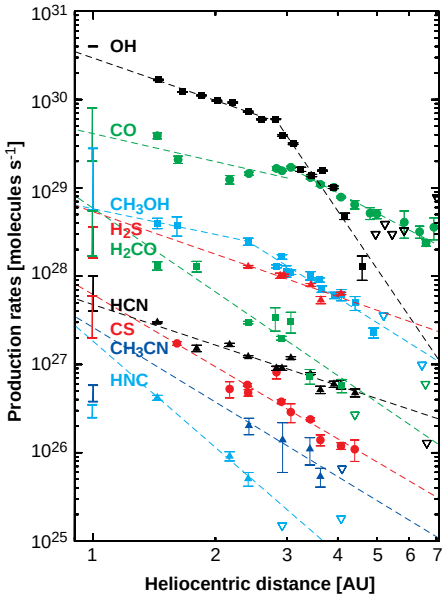


**Fig. 3.** Evolution of the molecular production rates with heliocentric distance $r_h$. Filled symbols with error bars correspond to detections; open triangles are upper limits. Exponents of the power-law fits: OH (black squares), −1.60 ± 0.03 ($r_h$ < 2.8 AU) and −6.79 ± 0.35 ($r_h$ > 2.8 AU); CO (green circles), −1.05 ± 0.13 ($r_h$ < 3.1 AU) and −2.39 ± 0.06 ($r_h$ > 3.1 AU); $CH_3OH$ (blue squares), −0.96 ± 0.02 ($r_h$ < 2.4 AU) and −2.90 ± 0.12 ($r_h$ > 2.4 AU); $H_2S$ (red triangles), −1.60 ± 0.14; $H_2CO$ (green squares), −3.15 ± 0.18; HCN (black triangles), −1.52 ± 0.06; CS (red circles), −2.71 ± 0.15; $CH_3CN$ (dark blue triangles), −2.8 ± 0.3; and HNC (blue triangles), −3.99 ± 0.06. The vertical bars at $r_h$ = 1 AU correspond to the ranges of molecular abundances measured in previous comets near perihelion (*1*). The scaling was made assuming an OH production rate of 4 × $10^{30}$ molecules per second for Hale-Bopp at perihelion.

outflow velocities of $H_2O$ and the other observed species show about the same trends.

Another basic parameter needed to derive production rates from rotational line intensities is the kinetic temperature of the gas. Simultaneous observations of several lines of the same molecule allow one to calculate the rotational temperature of the observed species averaged over the beam. In the inner coma, collisional excitation prevails, and the rotational temperature reflects the kinetic temperature, but in the outer coma, the rotational temperature is determined by radiative excitation. Calculations show that the CO transitions and the $CH_3OH$ lines at 304 to 307 GHz or around 157 GHz act as good thermometers, providing rotational temperatures close to the kinetic temperature within a few kelvin. This is not the case for the HCN lines and the groups of $CH_3OH$ lines around 145, 242, and 252 GHz, whose level populations relax rapidly to fluorescence equilibrium. The gas kinetic temperature increased from about 10 to 65 K from 6.6 to 1.4 AU, roughly as $r_h^{-1}$ (Fig. 2C).

For most species, the models used for converting line intensities into molecular production rates (*18*) take into account excitation through collisions and fluorescence. The size of the region where the OH 18-cm maser emission is quenched by collisions was constrained with the use of OH data taken at offset positions from the nucleus (*19*). The measured gas temperature (Fig. 2C) was used to compute the thermal population of the rotational levels in the collision-dominated coma (*18*). We used Haser density distributions (*20*) and did not consider the sublimation from grains or the asymmetry of the coma. We assumed that CS was produced by $CS_2$ and that $H_2CO$ was released from an extended source (*21*).

At $r_h \gtrsim 4$ AU, CO is the main driver of the activity of Hale-Bopp (Fig. 3). Another significant contributor, not observable at radio wavelengths, is $CO_2$ (*10*). The $H_2O$, released from grains, and the other volatiles studied here only contribute weakly to the comet's activity at $r_h \gtrsim 4$ AU. As Hale-Bopp approached the sun, molecular species displayed different behaviors in their production rate. At $r_h \gtrsim 2.8$ AU, OH (that is, $H_2O$) showed a steep variation in production rate roughly as $r_h^{-6.8}$ and a slower increase as $r_h^{-1.6}$ at $r_h < 2.8$ AU. At about 3 AU, the $H_2O$ production rate began to exceed that of CO, marking a change from a CO-driven coma to an $H_2O$-driven coma. A temporary stagnation is seen for OH between 3.7 and 3.2 AU, which probably reflects the disappearance of $H_2O$ ice grains in the coma and the onset of effective $H_2O$ sublimation from the nucleus, as expected from modeling (*22*). The heliocentric total visual magnitudes also show a plateau at the same $r_h$'s, which may be related to the change of regime from dust dragged by CO to dust dragged by $H_2O$. The heliocentric variation of the $H_2O$ production rate observed between 1.4 and 2.8 AU is close to the $r_h^{-2}$ dependence predicted by heat flow models at these distances (*23*).

After $H_2CO$ (*24*), CS, $CH_3CN$, and $CH_3OH$ were first observed in the comet, their production rates rose rapidly, roughly as $r_h^{-3}$. The production rates of CO, $H_2S$, and HCN increased more slowly, with slopes between $r_h^{-1.5}$ and $r_h^{-2.4}$. Our marginal detections and upper limits suggest that the onset of outgassing of $CH_3OH$ and HCN was more rapid than their subsequent evolution. As Hale-Bopp approached 3 AU, the evolution of the outgassing of some species changed, as for $H_2O$. The CO production rate stagnated and then rose again at $r_h \sim 2$ AU. The $CH_3OH$ production rate increased more slowly. The rate of HNC production showed a steep evolution as $r_h^{-4}$ since its detection at $r_h = 2.4$ AU (Table 1).

We would expect the more volatile species to be relatively more abundant in the coma far from the sun. Although there are differences with molecular abundances measured in other comets at $r_h \sim 1$ AU, there is no simple correlation between overabundance and volatility (defined by the sublimation temperature of the pure ices). The most volatile species, CO and $H_2S$, are indeed overabundant in Hale-Bopp at 4 AU, but HCN, which is also overabundant, has the same sublimation temperature as $CH_3CN$ and $CH_3OH$, both found with normal ratios at this distance. These differences presumably reflect the number of physicochemical processes taking place inside a comet nucleus as a result of solar heating, causing chemical differentiation. A thermodynamic model was used to simulate the evolution of the $H_2O$ and CO production rates in Hale-Bopp (*12*). When $H_2O$ ice is amorphous, this model is able to explain the CO production rate measured at $r_h > 3$ AU with a CO source underneath the comet's surface. This model predicts the stagnation seen at 3 AU, due to the increasing depth of the CO sublimation front. It also predicted the increase in CO seen at $r_h \sim 2$ AU, due to the decrease of the depth of CO sublimation resulting from surface erosion caused by $H_2O$ sublimation.

As $r_h$ decreased, the relative molecular production rates approached those found in other comets near 1 AU (*1*). This indicates that, in terms of chemical composition, Hale-Bopp is a typical comet. The notable exception is HNC. This unstable species was detected in Hyakutake at $r_h = 1$ AU (*25*) with a relative abundance to HCN of 6%. It was argued that the strong similarity of the HNC/HCN ratio in comets to those observed in warm quiescent molecular clouds suggests that cometary nuclei are composed of relatively unprocessed molecular ices. This ratio was less than 2% in Hale-Bopp at 2.9 AU and increased up to 20% at 1.4 AU. Although little is known about the thermodynamic properties of HNC ices, these strong variations cast doubt on the true value of the HNC/HCN ratio in cometary nuclei. The similarity of the heliocentric evolution of the HNC outgassing with that of $H_2CO$ (*24*), known to be produced from an extended source in the coma rather than from the nucleus (*21*), might argue against a nuclear origin.

**Table 1.** Observed molecular species with approximate dates of the first unambiguous detection with corresponding $r_h$ and the main frequencies at which each was observed in the present work.

| Species | First detection | | | Main frequencies observed (GHz) |
|---|---|---|---|---|
| | Date | $r_h$ (AU) | Ref. | |
| CO | September 1995 | 6.9 | (*6, 22*) | 115.3, 230.5, 345.8, 461.0 |
| $CH_3OH$ | March 1996 | 4.9 | (*28*) | 97,* 145,* 157,* 242,* 252,* 304.2, 307.2 |
| HCN | April 1996 | 4.8 | (*29*) | 88.6, 265.9, 354.5 |
| OH | April 1996 | 4.7 | (*30*) | 1.612, 1.665, 1.667, 1.720 |
| $H_2S$ | May 1996 | 4.3 | (*31*) | 168.7 |
| $H_2CO$ | June 1996 | 4.1 | (*32*) | 218.2, 225.7, 351.8 |
| CS | June 1996 | 4.1 | (*32*) | 98.0, 147.0, 244.9, 342.9 |
| $CH_3CN$ | August 1996 | 3.4 | (*33*) | 147.1* |
| HNC | November 1996 | 2.4 | (*34*) | 90.6, 272.0 |

*Multiple transitions observed.

## REFERENCES AND NOTES


1. D. Bockelée-Morvan, in *Molecules in Astrophysics: Probes and Processes*, E. van Dishoeck, Ed. (IAU Symp. 178, Kluwer Academic, Dordrecht, Netherlands, in press).
2. M. C. Senay and D. Jewitt, *Nature* **371**, 229 (1994); J. Crovisier *et al.*, *Icarus* **115**, 213 (1995).
3. A. Hale and T. Bopp, *IAU Circular 6187* (1995).
4. The half-power beam width (HPBW) of the IRAM antenna is 10 arc sec at 230 GHz and 26 arc sec at 89 GHz. Most of the spectra were acquired at a spectral resolution of 20 to 40 kHz, corresponding to

velocities of 0.026 to 0.052 km $s^{-1}$ at 230 GHz. Whenever possible, a frequency-switching mode was used.
5. The HPBW of the JCMT antenna is 14 arc sec at 345 GHz. Most data were obtained in the 300- to 370-GHz window with a spectral resolution of 95 kHz, in the frequency-switching mode.
6. N. Biver *et al.*, *Nature* **380**, 137 (1996).
7. Observations with the Nançay radio telescope (right ascension × declination of the HPBW was 3.5 arc min × 19 arc min) were undertaken with the technique previously used for comet P/Halley and other comets [E. Gérard, D. Bockelée-Morvan, G. Bourgois, P. Colom, J. Crovisier, *Astron. Astrophys. Suppl. Ser.* **77**, 278 (1989)].
8. A. Wootten *et al.*, *IAU Circular 6362* (1996); L. M. Woodney, J. McMullin, M. F. A'Hearn, *IAU Circular 6344* (1996); D. C. Lis *et al.*, in preparation; D. C. Lis *et al.*, *IAU Circular 6362* (1996).
9. H. A. Weaver *et al.*, *IAU Circular 6376* (1996).
10. J. Crovisier *et al.*, *Astron. Astrophys.* **315**, L385 (1996); J. Crovisier *et al.*, *Science* **275**, 1904 (1997).
11. J. K. Davies *et al.*, *Icarus*, in press.
12. A. Enzian, thesis, Université Joseph Fourier, Grenoble, France (1997).
13. One cannot yet exclude asymmetric collisional quenching (related to higher densities in the antisolar direction) as a contributor to the persistent blueshift observed for OH at $r_h < 2.5$ AU. Detailed modeling is needed to examine whether this effect is significant.
14. P. Eberhardt *et al.*, *Astron. Astrophys.* **187**, 481 (1987).
15. When the outgassing is isotropic, the width of the parent molecule radio line at half intensity is close to twice the gas expansion velocity. The lines observed in comet Hale-Bopp indicate preferential outgassing toward Earth. Hence, the outflow velocity can be only estimated from the blue wing of the profile.
16. D. Bockelée-Morvan, J. Crovisier, E. Gérard, *Astron. Astrophys.* **238**, 382 (1990). The OH ejection velocity was assumed to be 1.05 km $s^{-1}$ [J. Crovisier, *ibid.* **213**, 459 (1989)].
17. F. P. Schloerb, W. M. Kinzel, D. A. Swade, W. M. Irvine, *Astron. Astrophys.* **187**, 475 (1987).
18. Molecule: model. OH: (*16*); linear molecules: J. Crovisier, *Astron. Astrophys. Suppl. Ser.* **68**, 223 (1987); $CH_3OH$: D. Bockelée-Morvan, J. Crovisier, P. Colom, D. Despois, *Astron. Astrophys.* **287**, 647 (1994); $H_2S$: J. Crovisier, D. Despois, D. Bockelée-Morvan, P. Colom, G. Paubert, *Icarus* **93**, 246 (1991); $H_2CO$: D. Bockelée-Morvan and J. Crovisier, *Astron. Astrophys.* **264**, 282 (1992). We assumed a total collisional cross section of $5 \times 10^{-14}$ $cm^2$. A pure thermal model was used for $CH_3CN$.
19. The quenching radius $r_q$ was estimated to have been $\sim 2.6 \times 10^5$ km in October and November 1996 at $r_h = 2.2$ to 2.7 AU, determined using the center exposure and the average east-west offset positions at 7 and 14 arc min, as in comet Hyakutake [E. Gérard *et al.*, in preparation]; the quenching was modeled according to $r_q = r_q^0 r_h (Q_{OH})^{0.5}$ [F. P. Schloerb, *Astrophys. J.* **332**, 524 (1988)], with $r_q^0 = 40{,}000$ km, $r_h$ in astronomical units, and the OH production rate $Q_{OH}$ in units of $10^{29}$ $s^{-1}$. We used the OH lifetime computed at solar minimum [S. A. Budzien, M. C. Festou, P. D. Feldman, *Icarus* **107**, 164 (1994)].
20. Haser molecular density distributions assume isotropic outflow at constant velocity. Production rates calculated with a more realistic angular density distribution are at most 15% higher.
21. The scale length of the $H_2CO$ parent is assumed to be 1.2 times the photodissociative scale length of $H_2CO$, as measured in comet P/Halley [R. Meier, P. Eberhardt, D. Krankovsky, R. Hodges, *Astron. Astrophys.* **277**, 677 (1993)].
22. D. Jewitt, M. Senay, H. Matthews, *Science* **271**, 1110 (1996).
23. A. H. Delsemme, in *Comets*, L. L. Wilkening, Ed. (Univ. of Arizona Press, Tucson, AZ, 1982), pp. 85–130.
24. The $H_2CO$ production rate computed under the assumption of direct release from the nucleus varies as $r_h^{-4.5}$. It is 0.2 to 0.7 times the $H_2CO$ production rate computed by assuming an extended source.
25. W. M. Irvine *et al.*, *Nature* **382**, 418 (1996).
26. R. M. Lees, *Astrophys. J.* **184**, 763 (1973).
27. The interpretation of line shifts and the comparison of line shifts of different species observed with different fields of view must be done with caution because the molecular coma is generally resolved by the beam of the radio telescope, and a fraction of molecules with small projected velocities are not seen by the instrument. In the case of outgassing restricted to the hemisphere toward Earth, we estimated that the millimeter lines are more blueshifted than the OH lines by about 0.05 km $s^{-1}$. In the present study of the OH velocity shifts (Fig. 2A), we did not consider spectra obtained from September to mid-October 1996, which suffered from OH contamination from the galactic plane. The scatter in the $H_2O$ expansion velocity (Fig. 2B) may be partly due to OH galactic contamination and the inability of the trapezium method to interpret asymmetric lines.
28. M. Womack *et al.*, *IAU Circular 6382* (1996); N. Biver *et al.*, *IAU Circular 6386* (1996).
29. D. Jewitt, M. Senay, H. Matthews, *IAU Circular 6377* (1996).
30. J. Crovisier *et al.*, *IAU Circular 6394* (1996).
31. L. M. Woodney *et al.*, *IAU Circular 6408* (1996).
32. N. Biver *et al.*, *IAU Circular 6421* (1996).
33. N. Biver *et al.*, *IAU Circular 6458* (1996).
34. D. Bockelée-Morvan *et al.*, *IAU Circular 6511* (1996).
35. The JCMT is operated by The Joint Astronomy Centre on behalf of the Particle Physics and Astronomy Research Council of the United Kingdom, the Netherlands Organisation for Scientific Research, and the National Research Council of Canada. The Nançay Radio Observatory is operated by the Unité Scientifique de Nançay of the Observatoire de Paris, associated as Unité de Service et de Recherche (USR) B704 to CNRS. The Nançay Observatory also gratefully acknowledges the financial support of the Conseil Régional of the Région Centre in France. This research has been supported by the Programme National de Planétologie de l'Institut National des Sciences de l'Univers and CNRS (URA 1757).

13 February 1997; accepted 6 March 1997

# The Spectrum and Spatial Distribution of Cyanogen in Comet Hale-Bopp (C/1995 O1) at Large Heliocentric Distance

R. Mark Wagner* and David G. Schleicher

Optical spectra of comet Hale-Bopp (C/1995 O1) at a heliocentric distance of 6.45 astronomical units showed emission from cyanogen gas. The spatial distribution of cyanogen was considerably more diffuse and extended compared to the spatial profile of the dust or grains which were sharply peaked near the center. This behavior is consistent with comets at smaller heliocentric distances suggesting the same or a similar formation mechanism. A cyanogen gas production rate of $(1.2 \pm 0.3) \times 10^{26}$ molecules per second was derived. A model band profile derived from fluorescence equilibrium calculations for the comet's heliocentric velocity and distance agrees with the observed band profile.

Comet Hale-Bopp (C/1995 O1) was discovered on 23 July 1995 at an integrated visual magnitude of ~11 (*1*) and at a heliocentric distance, $r_h$, of 7 astronomical units (AU) (*2*). The discovery of a luminous periodic comet at such a large distance from the sun initiated observations at optical and radio wavelengths to understand the physical and chemical processes occurring in the nucleus and coma which are not available from observations at smaller $r_h$. In particular, Fitzsimmons and Cartwright (*3*) detected emission from the CN (0-0) band in Hale-Bopp's coma at $r_h = 6.82$ AU; the second most distant reported detection for a comet (*4*, *5*).

Our observations of Hale-Bopp were obtained on 13.1 October 1995 universal time (UT) ($r_h = 6.45$ AU; 6.64 AU from Earth) with the 4.5-m Multiple Mirror Telescope and the blue channel charge-coupled device spectrograph (*6*). We obtained two 20-min exposures of Hale-Bopp with the spectrograph slit centered on the nucleus throughout the observation and oriented along the parallactic angle of 29° to minimize any loss of light due to atmospheric refraction. The position angle of the sun on the plane of the sky was 270° so that the slit was oriented nearly orthogonal to sun-tail direction on the sky. The spectrum of a solar analog star (van Bueren 64) was obtained to remove the reflected solar spectrum from the comet spectrum. The first comet exposure was heavily contaminated by background stars and was discarded.

The data were reduced and processed using standard procedures (*7*). Because any gas coma of Hale-Bopp is expected to be quite extended and probably even extends beyond the bounds of our short slit, sky subtraction was accomplished by first inter-

R. M. Wagner, Department of Astronomy, The Ohio State University, 174 West 18th Avenue, Columbus, OH 43210, USA, and Lowell Observatory, 1400 West Mars Hill Road, Flagstaff, AZ 86001, USA.
D. G. Schleicher, Lowell Observatory, 1400 West Mars Hill Road, Flagstaff, AZ 86001, USA.

*To whom correspondence should be addressed. E-mail: rmw@lowell.edu